Multi-mode Dynamic Proportional Energy Management Strategy for Battery-Supercapacitor Hybrid Energy Storage System of Tram Based on Pseudo-spectrum Method

Xingkun An
Dept. of Electrical Engineering
Beijing Jiaotong University
Beijing, China
17121411@bjtu.edu.cn

Zhongping Yang
Dept. of Electrical Engineering
Beijing Jiaotong University
Beijing, China
zhpyang@bjtu.edu.cn

Yu Wang
Dept. of Electrical Engineering
Beijing Jiaotong University
Beijing, China
16117402@bjtu.edu.cn

Fei Lin
Dept. of Electrical Engineering
Beijing Jiaotong University
Beijing, China
flin@bjtu.edu.cn

Feng Li
Dept. of Electrical Engineering
Beijing Jiaotong University
Beijing, China
17126003@bjtu.edu.cn

Hongda Zhou
Dept. of Electrical Engineering
Beijing Jiaotong University
Beijing, China
14291262@bjtu.edu.cn

***Abstract*—In this paper, a self-adaptive multi-mode dynamic proportional control strategy for hybrid-energy-storage tramcar is proposed. With battery life and system efficiency as optimization objectives, power distribution between two sources is carried out by pseudo-spectral method. According to the optimization results, an on-line dynamic proportional EMS is extracted. Furthermore, in order to make the control strategy change with the actual situation, the EMS is improved to a self-adaptive dynamic proportional EMS. The simulation results show that compared with the traditional proportional control strategy, the multi-mode dynamic proportional control strategy greatly improves the battery life and efficiency.**

Keywords—hybrid energy storage; first-order model; energy management strategy; dynamic proportional control; pseudo-spectral method

I. INTRODUCTION

Trams are environmentally friendly, energy-saving and relatively inexpensive. They are suitable in medium-sized cities. At present, the power source of most tramcar is traction network. On the one hand, the erection of traction network affects the beauty of the city, on the other hand, the initial investment of traction network is large and the construction cycle is long. In recent years, with the implementation of clean energy policy and the demand for safety and aesthetics of public transportation, energy-storage trams have begun to emerge and been widely studied, gradually replacing traction-net trams.

Lithium batteries and supercapacitors are the main energy storage components commonly used in trams. Lithium batteries have high energy density and low power density, while supercapacitors have high power density and low energy density. Their characteristics complement each other. In recent years, hybrid energy storage system (HESS) which combines them has been applied more and more widely [1], but HESS increases the complexity of control. More and more attention has been paid to the research of energy management strategy (EMS), which is how to distribute the required power between lithium batteries and supercapacitors for trams.

The energy management strategies applied to the HESS of trams can be roughly divided into heuristic methods and optimization methods. Heuristic methods can realize real-time control, such as neural network ([2] ,[3]), fuzzy control [4], rule control [5] and so on. For the rule control method, there are a lot of studies using genetic algorithm to optimize the parameters of the rule control ([6]-[9]), which makes the rule control strategy more effective. The optimization method is based on the objective function ([10]-[13]) to optimize the power distribution, which can not achieve the purpose of real-time control. The commonly used optimization method ([14] ,[15]) is dynamic programming [16], but the accuracy of the optimization results is affected by the discrete degree of state variables, and the running time is long. Moreover, the accurate battery model brings more complexity and challenges to the optimization of power distribution, because too many state variables will lead to "dimension disaster" in DP, which greatly increases the computing time. For avoiding these shortcomings, the pseudo-spectral method ([17]-[18]) is used to optimize the power distribution strategy. In order to avoid the non-optimality of the heuristic methods and the non-real-time performance [19] of the optimization methods, the results obtained by the pseudospectral method are extracted into an online dynamic proportional control strategy.

The structure of this paper is as follows: In section II, the model of HESS is established, the influencing factors of battery life are briefly described, and the capacity attenuation model of battery is put forward. In section III, based on the objective functions, the optimal control sequence is calculated by pseudo-spectral method, and the dynamic proportional control (DPC) strategy is extracted from the optimal control sequence. In section IV, according to the typical power between two stations of a domestic tram line, the DPC is obtained by using the method proposed in section III, and the control results of DPC, PSC (pseudo-

The National Key Research and Development Program of China (No. 2017YFB1201105).

978-1-7281-2124-6/19/$31.00 ©2019 IEEE

spectral control) and OPC (optimal proportional control) are compared.

II. System Modeling

A. Component Modeling

The HESS of tramcar consists of lithium titanate batteries and supercapacitors. The semi-active topology of batteries is adopted, that is, batteries are connected to DC buses in parallel through DC/DC converters, and supercapacitors are connected to DC bus directly, as shown in Fig. 1.

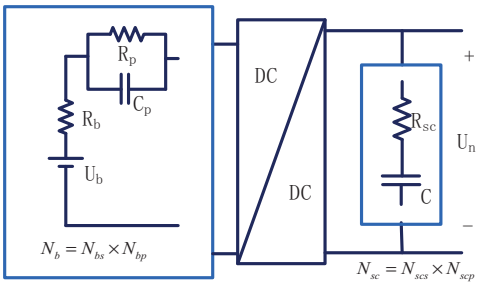

Fig. 1. Topological structure of HESS

Supercapacitor has high power density, so it takes on high power output and absorption. Compared with the dual DC/DC topology, the batteries semi-active topology can reduce the power level of the converter, reduce the volume and weight of the whole HESS, and reduce the energy loss on the DC/DC converter.

The model of supercapacitor is shown in Fig. 1. *C* is the equivalent capacitance of supercapacitor and *Rsc* is its internal resistance.

The first-order model of lithium battery is shown in Fig. 1. U_b is the open-circuit voltage, R_b and R_p are ohmic internal resistance and polarization internal resistance respectively. C_p is the polarization capacitor of the battery. The parameters of the battery vary with the change of SOC.

B. Cyclic Life Model of LTO Batteries

The establishment of LTO battery cycle life model is of great significance for predicting the capacity loss of LTO lithium battery. The experimental data is very important for the research and validation of battery cycle life model. However, few literatures have established LTO battery life model based on a large number of experiments. Compared with traditional batteries such as lithium iron phosphate batteries and ternary lithium batteries, LTO batteries are a new type of batteries. The research is not deep enough. Moreover, the life of LTO batteries is much longer than that of traditional batteries, and the experiments will be costly and laborious. This paper simplifies the life model, assuming that the temperature management module of HESS can control the temperature well at the appropriate temperature of 25 ℃.

In [20], [21], it is mentioned that for traditional batteries, the increase of C-rate will increase the capacity attenuation rate of batteries. However, it can be found in the battery technical manual that the effect of the magnitude of the current on the life of LTO batteries is not significant. Therefore, the ampere-hour integral method is used to evaluate the battery life attenuation. In order to quantify the battery life attenuation rate, it was analyzed by using the data from battery technical manual.

This research is based on a brand of 20Ah lithium titanate batteries. Based on the technical manual of the battery, the batteries capacity attenuation curves of 1C-rate and 3C-rate are drawn in Fig. 2. It can be seen that the magnitude of the current has little effect on the battery life. In the suitable C-rate range, it can be considered that the battery is insensitive to C-rate. The appropriate C-rate range given in the technical manual is [-5C, 5C].

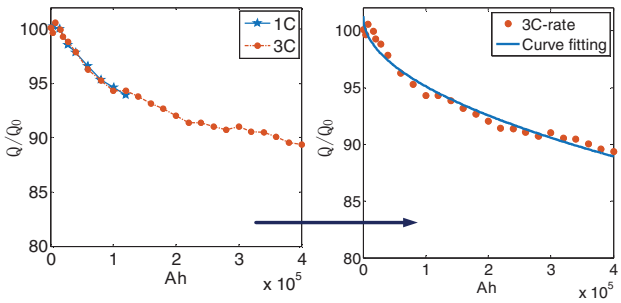

Fig. 2. Capacity attenuation curve for 20Ah lithium titanate battery

$$\frac{Q}{Q_0}(\%) = 100 - B \cdot e^{-E_a/RT} \cdot Ah^{\alpha} \tag{1}$$

$$Ah = \int |I_b| dt \tag{2}$$

where Q denotes the actual recyclable capacity of the battery, Q_0 denotes the initial recyclable capacity of the battery, and Ah denotes the accumulative ampere-hour throughput of the battery. [22] points out that the rate of capacity attenuation of LTO batteries is proportional to $\sqrt{Ah}$, i.e. α=0.5; at 25 ℃, the life model of LTO batteries can be obtained by fitting the capacity attenuation data of batteries.

$$\frac{Q}{Q_0}(\%) = 100 - 0.01955 \cdot Ah^{0.5} \tag{3}$$

When the battery cycles 20,000 times, that is, the accumulated throughput of Ah reaches 800 kAh, the recyclable capacity of the battery decreases to 82.5% of the initial capacity. Considering model errors, it is believed that the battery cycles 20,000 times to end of life.

Equation (4) is an expression for calculating the conversion cost of battery life attenuation. Because the capacity attenuation rate of LTO battery is proportional to $\sqrt{Ah}$, the attenuation rate of battery capacity will slow down with time. In a small time range, we can take the slope of the capacity attenuation curve as the current battery attenuation rate. The life damage conversion cost of LTO batteries can be expressed as follows:

$$C_1 = k \int \frac{|I_b|}{2n_b \times Q_0 \times 3600} (C_b \times N_b)\, dt \tag{4}$$

where k is a coefficient related to temperature and SOH of batteries, C_b is the unit price of batteries, N_b is the number of batteries, n_b = 20000, indicating the number of cycles to the end of life.

III. Optimization of EMS

A. Establishment of Objective Function

The establishment of objective function is very important for optimizing EMS. The objective function includes two factors: battery life and system efficiency. In order to convert these two objectives into a comprehensive index as the objective function, the battery life and system efficiency are all converted into costs, and then the two factors are combined as the objective function after unification, as shown in (6).

$$C_2 = \frac{\int_0^{t_f} (I_b^2 R_b + I_p^2 R_p) N_b + I_{sc}^2 R_{sc} N_{sc} + P_{DC} dt}{3600 \times 1000} C_e \tag{5}$$

$$C = C_1 + C_2 \tag{6}$$

where I_b and I_P are terminal current and polarization resistance current of lithium batteries, R_b and R_p are ohmic internal resistance and polarization internal resistance of batteries, I_{sc} is the current of supercapacitors, R_{sc} is the internal resistance of supercapacitors, P_{DC} is the loss power of DC/DC converter, C_e is the unit price of electricity.

B. Determination of Initial Condition

The initial condition of problem refers to the initial SOC of supercapacitors, that is, the initial voltage. On the way of tram, charging stations will be installed at some stations to replenish the HESS of tramways in time. Charging stations can charge batteries and supercapacitors by different control strategies. What we need to think about is how high the supercapacitor should be charged at the charging station, which is the best for the system. In order to compare the influence of different initial SOC of supercapacitor on HESS, two different hybrid energy storage systems 1 and 2 with different *SOCsc_init* are considered. The initial voltage of supercapacitor of system 2 is set to be high:

$$U_{sc\_init1} \le U_{sc\_init2} \tag{7}$$

Using the same control strategy (such as threshold method), the supercapacitors of the two systems share the same power value at a certain time.

The efficiency of the two systems is analyzed by mathematical induction. Suppose at (*k-1*) time, the supercapacitor voltage of system 2 is higher than that of system 1:

$$U_{sc1}(k-1) \le U_{sc2}(k-1) \tag{8}$$

The supercapacitor terminal current expression is:

$$I_{sc} = \frac{U_{sc} - \sqrt{U_{sc}^2 - 4R_{sc}P_{sc} / N_{sc}}}{2R_{sc}} \tag{9}$$

The supercapacitor current expression derives the supercapacitor voltage.

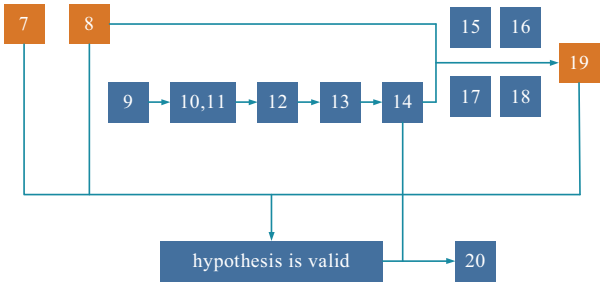

Fig. 3. The process of mathematical induction

$$\dot{I}_{sc} = \frac{1}{2R_{sc}}\left(1 - \frac{U_{sc}}{\sqrt{U_{sc}^2 - 4R_{sc}P_{sc} / N_{sc}}}\right) \tag{10}$$

$$\dot{I}_{sc} \begin{cases} < 0, P_{sc} > 0 \\ = 0, P_{sc} = 0 \\ > 0, P_{sc} < 0 \end{cases} \tag{11}$$

From the above analysis, it can be concluded that: when $P_{sc} > 0$, the higher the U_{sc}, the smaller the I_{sc}; if $P_{sc} < 0$, the higher the U_{sc}, the larger the I_{sc}, for I_{sc} is negative, the smaller $|I_{sc}|$, that is:

$$\left|I_{sc1}(\mathrm{k}-1)\right| \ge \left|I_{sc2}(\mathrm{k}-1)\right| \tag{12}$$

Because the loss of supercapacitor is:

$$P_{sc\_loss} = N_{sc} I_{sc}^2 R_{sc} \tag{13}$$

Therefore,

$$P_{sc\_loss1}(\mathrm{k}-1) \ge P_{sc\_loss2}(\mathrm{k}-1) \tag{14}$$

According to the expression of U_{sc}, the voltage of supercapacitor at k time satisfies:

When supercapacitor discharges:

$$U_{sc\_dis}(k) = U_{sc}(k-1) - \Delta U_{sc\_dis}(k) \tag{15}$$

$$\Delta U_{sc\_dis}(k) = \sqrt{\frac{2(P_{sc}(k\text{-}1) + P_{sc\_loss}(k\text{-}1))T(k\text{-}1)}{C}} \tag{16}$$

When the supercapacitor is charged:

$$U_{sc\_cha}(k) = U_{sc}(k-1) + \Delta U_{sc\_cha}(k) \tag{17}$$

$$\Delta U_{sc\_cha}(k) = \sqrt{\frac{\text{-}2(P_{sc}(k\text{-}1) + P_{sc\_loss}(k\text{-}1))T(k\text{-}1)}{C}} \tag{18}$$

It can be inferred that:

$$U_{sc1}(k) \le U_{sc2}(k) \tag{19}$$

Assumption stands, it can be inferred that:

$$\sum_{1}^{kf} P_{sc\_loss1}(k) \ge \sum_{1}^{kf} P_{sc\_loss2}(k) \tag{20}$$

where k_f refers to the total number of discrete time of the whole journey. Obviously, under the same control strategy, the higher the initial voltage, the smaller the loss and the higher the efficiency.

Fig. 3 is the process of mathematical induction, where the numbers indicate the number of the expression and the arrows indicate the direction of the derivation. Based on the above analysis, the optimal initial condition of the problem is determined, that is, the initial SOC of supercapacitor is 1. Based on the initial condition, the optimization problem is established.

C. Establishment of Optimization Problem

Through traction calculation, the power data P can be obtained. P is the input variable of the optimization problem. the control variable of power distribution is u, and u represents the ratio of the power allocated to the battery to the total power. The optimization problem is to find the optimal control variable to make the objective function optimal in the case of the given input variable. The state variables are SOC_b of the battery, voltage of the supercapacitor U_{sc} and polarization resistance current I_p of the battery, where the control variable and the input variable are respectively k_f-dimensional vectors

$$u = (u(1), u(2), ..., u(k_f)) \tag{21}$$

$$P = (P(1), P(2), ..., P(k_f)) \tag{22}$$

When the input variable P is known, the power of the battery and the supercapacitor is set as(23),(24):

$$P_b = \begin{cases} \eta \cdot u \cdot P, P \le 0 \\ \dfrac{u \cdot P}{\eta}, P > 0 \end{cases} \tag{23}$$

$$P_{sc} = P(1-u) \tag{24}$$

In (23), (24), η refers to the efficiency of DC/DC converter.

Then the current of the battery and the supercapacitor can be calculated as follows:

$$I_b = \frac{(U_b - I_p R_p) - \sqrt{(U_b - I_p R_p)^2 - 4 R_b P_b / N_b}}{2 R_b} \tag{25}$$

$$I_{sc} = \frac{U_{sc} - \sqrt{U_{sc}^2 - 4 R_{sc} P_{sc} / N_{sc}}}{2 R_{sc}} \tag{26}$$

Then the differential equations of state variables SOC_b, U_{sc} and I_P are constructed:

$$\dot{SOC}_b = -\frac{I_b}{3600 Q_0} \tag{27}$$

$$\dot{U}_{sc} = -\frac{I_{sc}}{C} \tag{28}$$

$$\dot{I}_p = \frac{I_b - I_p}{\tau} \tag{29}$$

$$\tau = R_p \times C_p \tag{30}$$

Loss power of DC/DC converter is a function of input variable P and control variable u.

$$P_{DC} = \begin{cases} uP(\dfrac{1}{\eta} - 1), P \ge 0 \\ uP(\eta - 1), P < 0 \end{cases} \tag{31}$$

In the optimization problem, we need to add restrictions on state variables SOC_b and U_{sc}, control variable u, and path restrictions, i.e. the limits of I_b and I_{sc}.

$$\begin{cases} I_{b\_\min} \le I_b \le I_{b\_\max} \\ SOC_{b\_\min} \le SOC_b \le SOC_{b\_\max} \\ I_{\mathrm{sc}\_\min} \le I_{sc} \le I_{\mathrm{sc}\_\max} \\ U_{\mathrm{sc}\_\min} \le U_{sc} \le U_{\mathrm{sc}\_\max} \\ 0 \le u \le 1 \end{cases} \tag{32}$$

The above objective function (6), state differential equations (27), (28), (29), equality constraints (23), (24), (25), (26), state constraints and path constraints inequalities (32) together constitute a trajectory optimization problem. In this optimization problem, it is necessary to find an optimal sequence of control variable u in the case of a given input variable sequence P. In order to find the optimal result, the pseudo-spectral method is used to solve the optimization problem.

D. Pseudo-spectral Method

The essence of EMS is power allocation method. Power allocation is a trajectory optimization problem. Pseudo-spectral method can be used to optimize the trajectory optimization problem. The pseudo-spectral method is briefly introduced below. The standard form of trajectory optimization is:

$$C = \int_{t_0}^{t_f} \theta(x(t), u(t), t) dt \tag{33}$$

$$\dot{x}(t) = f(x(t), u(t), t) \tag{34}$$

$$p(x(t), u(t), t) \le 0 \tag{35}$$

$$x_{\min}(t) \le x(t) \le x_{\max}(t) \tag{36}$$

$$u_{\min}(t) \le u(t) \le u_{\max}(t) \tag{37}$$

Equation (33) is the objective function of the trajectory optimization problem. Equation (34) is a state differential equation. Equation (35) is a path-limited inequality. Equations (36), (37) are constraint inequalities of state variables and control variables.

Firstly, the time interval in trajectory optimization problem needs to be normalized to [-1,1], such as (38).Then

the LGR (Legendre-Gauss-Radau) collocation points are computed in the normalized interval. LGR collocation points are the zeros of sum of N-order Legendre polynomials and N+1-order Legendre polynomials.

$$t = \frac{t_f - t_0}{2}\tau + \frac{t_f + t_0}{2} \tag{38}$$

Radau pseudo-spectral method is used to solve the optimal control problem. The unknown state variables and control variables are discretized at the LGR point. The real state variables and control variables are approximated by Lagrange interpolation, and the approximate state variables are derived instead of the state differential equations. The optimal control problem is transformed into a discrete nonlinear programming problem.

The state variables and their differential and control variables are approximately as follows:

$$x(\tau) \approx X(\tau) = \sum_{i=1}^{N+1} L_{1,i}(\tau) X_i \tag{39}$$

$$\dot{x}(\tau_k) \approx \dot{X}(\tau_k) = \sum_{i=1}^{N+1} \dot{L}_{1,i}(\tau_k) X_i = \sum_{i=1}^{N+1} D_{k,i} X_i \tag{40}$$

$$u(\tau) \approx U(\tau) = \sum_{i=1}^{N} L_{2,i}(\tau) U_i \tag{41}$$

In (39), (40) and (41), X_i and U_i are the values corresponding to the state variable and the control variable at the collocation point, while $L_{1,i}$, $L_{2,i}$ are the Lagrange interpolation coefficients of the state variables and the control variable respectively.

By derivation and approximation, the trajectory optimization problem can be transformed into the following discrete nonlinear programming problems:

The objective function is transformed into:

$$C = \frac{t_f - t_0}{2} \sum_{k=1}^{N} \alpha_k \theta(X_k, U_k, \tau_k, t_0, t_f) \tag{42}$$

In (42):

$$\alpha_k = \frac{2}{(1-\tau_k^2)(\dot{P}_N(\tau_k))^2} \tag{43}$$

$$P_N = \frac{1}{2^N N!} \frac{d^N}{d\tau^N} (\tau^2 - 1)^N \tag{44}$$

Equation (34) is converted to:

$$\sum_{i=1}^{N+1} D_{k,i} X_i = \frac{t_f - t_0}{2} f(X_k, U_k, \tau_k, t_0, t_f) \tag{45}$$

Equation (35) is converted to:

$$p(X_k, U_k, \tau_k, t_0, t_f) \le 0 \tag{46}$$

By integrating the constraints, differential equations and objective function with the pseudo-spectral tool GPOPS-II in MATLAB [18], the comprehensive optimization problem of tram can be solved.

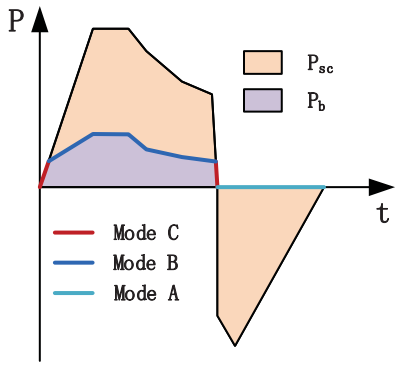

Fig. 4. The schematic diagram of multi-mode DPC strategy

E. Multi-mode DPC Strategy

The optimal control sequence obtained by pseudo-spectral method provides a very important reference for real-time control strategy. The online control rules can be extracted from the optimal control sequence. According to the range of u (0-1), the modes of DPC is divided into:

- A, u = 0, pure supercapacitor mode
- B, 0 < u< 1, dynamic proportion control mode
- C, u = 1, pure battery mode

Battery is a kind of high-energy-density storage component. The main function of battery in HESS is to provide energy. In order to reduce the ampere-hour integral throughput of battery and prolong the battery life as far as possible, during the braking process of tram, the braking energy is absorbed only by supercapacitors (mode A). In the traction stage, power distribution should take into account both the discharge rate of the battery in an appropriate range and the battery life, as well as the efficiency of the HESS. The control variable u will change with the change of the input variable P. With the increase of P, mode C will be switched to mode B. When traction power is small, the significance of providing all power by battery is to delay the supercapacitor to enter the low efficiency state, so as to improve the total efficiency of supercapacitor in the whole period. The efficiency of the supercapacitor is related to power and U_{sc}. In the case of equal power, the higher the voltage is, the higher the efficiency is.

The schematic diagram of the DPC is shown in Fig. 4.

IV. Case Study

A. Road Condition and Energy Storage Component

The batteries and supercapacitors used in the simulation are 20Ah lithium titanate batteries of a certain brand and 3000F supercapacitors of a certain brand respectively. Their parameters are as TABLE I. , in which the battery parameters are calculated based on the least square method in the HPPC experiment with SOC=0.7.

The simulation route is selected between a certain two stations on a Chinese tram line. By traction calculation, the power curve can be obtained as shown in Fig. 6.

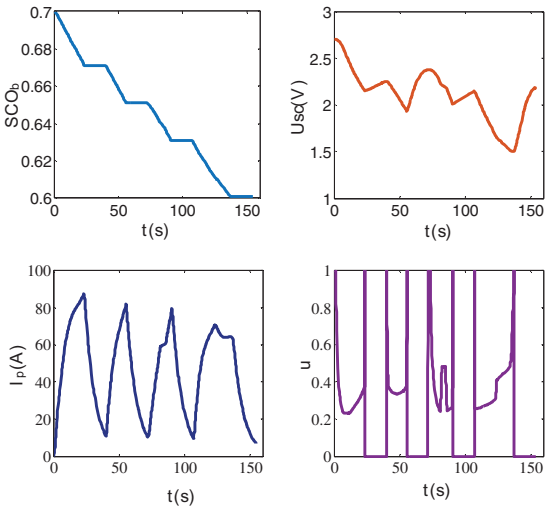

Fig. 5. Curves of state variables and control variable

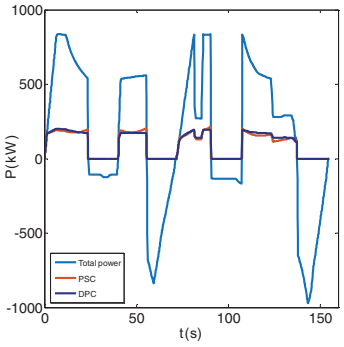

Fig. 6. Battery power curve based on PSC and DPC

TABLE I. ENERGY STORAGE COMPONENT PARAMETERS

Parameter	LTO battary	Supercapacitor
Rated Voltage (V)	2.359	2.7
Rated Capacity	20Ah	3000F
Internal Resistance (mΩ)	R_b=0.71， R_p=0.66	0.29
Maximum Current (A)	100(5C)	300
Mass (kg)	0.515	0.338
Cyclic Life (times)	20000	2000000
Capacity Configuration	186S6P	330S8P
Unit Price（¥）	400	390

B. Pseudo-spectral Simulation Results

According to section III , the power data, the constraints of state variables, differential equations, path constraints and objective function are input into the GPOPS-II toolbox, and the curves of state variables SOC_b, SOC_{sc}, I_P and control variable u varying with time are obtained as shown in Fig. 5.

The power curve of the battery obtained by pseudo-spectral method is shown in Fig. 6.

C. Real-time Control Strategy

In order to extract the relationship between the control variable u and the input variable P from the results of pseudo-spectral method, the power P and the corresponding optimized control variable are shown as horizontal and

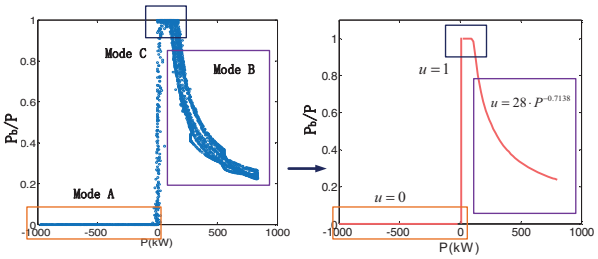

Fig. 7. Extraction of DPC

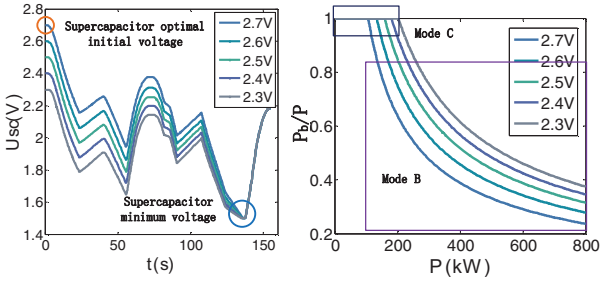

Fig. 8. SC voltage curves and Control curves of DPC under different SC initial voltages

vertical coordinates respectively in Fig. 7. Combining with the analysis in III.E, we can find that in Fig. 7, there are three parts, corresponding to mode A, C and B. In mode B, the relationship between control variable u and input variable P is fitted by least square method.

The power function $u = a \cdot P^{-b}$ is used to fit the relationship between proportion value and power value.

$$u = 28 \cdot P^{-0.7138} \tag{47}$$

In order to compare the DPC strategy and the optimal control strategy obtained by pseudo-spectral method, the battery power obtained by these two methods are compared in the same coordinate system, as shown in Fig. 6. It is found that the battery powers obtained by the two control strategies is almost the same, which proves that the DPC strategy is effective.

D. Adaptive Multi-mode DPC

When the optimized EMS is applied to the actual line, its initial condition (U_{sc_init}) or input condition (P) often change. based on the different initial voltage of supercapacitors and different traffic congestions, the power distribution strategy is re-optimized by using pseudo-spectral method.

When the tram arrives at the charging station, it can replenish energy in time. In III.B , the analysis shows that the most friendly initial condition for the HESS is to fill the supercapacitor. However, due to the limitation of charging strategy and charging time, the supercapacitor may not be full. When the supercapacitor initial voltages are different, the power distribution ratio is re-optimized by pseudo-spectral method. The optimized supercapacitor voltage curve is shown in Fig. 8. In Fig. 8, it can be seen that the voltage curves of the supercapacitor reach the minimum at the maximum energy consumption point of the tramcar, which shows that increasing the utilization rate of the supercapacitor can optimize the objective function and reduce the operation cost of the tramcar. The main purpose of increasing the utilization rate of supercapacitors is to

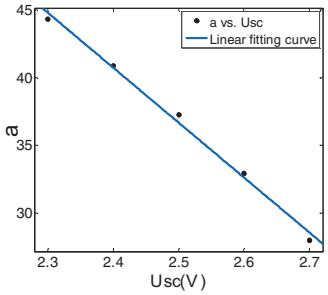

Fig. 9. Linear fitting of pre-exponential factor

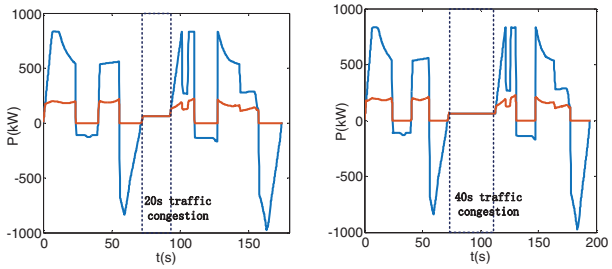

Fig. 10. Battery power curves of 20s /40s traffic congestion conditions

reduce the Ah throughput of batteries and prolong the life of batteries.

When the initial voltage of the supercapacitor is too low, the energy carried by the supercapacitor is too small, which causes the battery to bear more energy output, thus making the power of the battery too large. When the initial voltage is 2.3V, the maximum discharge rate of the battery has reached 7.5C, which is very harmful to the life of the battery. Therefore, when the initial voltage of the supercapacitor is lower than 2.3V, some measures should be taken to increase the initial voltage of the supercapacitor, such as extending the parking time at the charging station.

According to IV.C, the PSC is transformed into DPC, and the mode C and mode B in each case (2.7V, 2.6V, 2.5V, 2.4V and 2.3V) are drawn in the same coordinate system. In the case of different initial voltages, the control variable of mode B have the same trend with the input variable. Therefore, make b=-0.7138 in (48), the pre-exponential factor a is identified by least squares method. Fig. 8 shows the control proportion curve of DPC mode B under different voltages.

$$u = a \cdot P^{-b} \tag{48}$$

In order to make the control strategy adjust steplessly with different initial voltages, the pre-exponential factors of mode B under different voltages are searched, and the pre-exponential factors of mode B in 5 cases with 0.1 interval between 2.3V and 2.7V are linearly fitted as shown in Fig. 9, It can be deduced that:

$$a = -40.55U_{sc} + 138.1 \tag{49}$$

$$u = (-40.55\,\mathrm{U}_{sc} + 138.1) \cdot P^{-0.7138} \tag{50}$$

Before considering the impact of traffic congestion on DPC, the following two points should be made to enable you to better understand the following analysis:

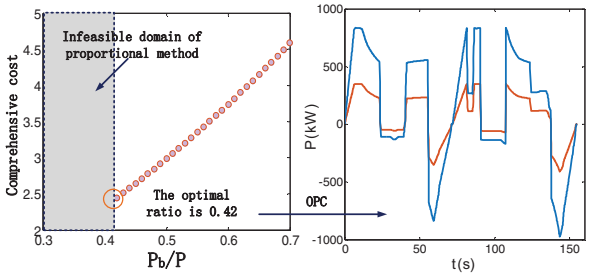

Fig. 11. Optimal proportional control

TABLE II. INDICATORS OF THREE CONTROL STRATEGIES

	Efficiency	Increase Percentage	Battery life (years)	Increase Percentage
OPC	89.48%	—	5.802	—
DPC	95.59%	6.83%	11.125	47.85%
PSC	96.59%	7.95%	11.330	48.79%

- A period of parking time is added to the power curve calculated to simulate the traffic congestion.
- When parking, the auxiliary power is 45 kW.

Fig. 10 is power of tramcar with simulated traffic congestion of 20s and 40s respectively. In both cases, the pseudo-spectral method is used to redistribute the power between the batteries and the supercapacitors. The power curves of battery are drawn in the Fig. 10. In the time interval outside the traffic congestion, the power distribution is exactly the same as the situation of IV.C. During the traffic congestion, the power is supplied by battery, that is, the HESS runs in mode C. Since 45 kW is within the power range of mode C, traffic congestion has no effect on power distribution. During the traffic congestion, the lithium batteries should provide all the auxiliary power.

E. Comparison and Analysis

Proportional method is one of the commonly used heuristic methods. The advantage of proportional method is that there is only one empirical parameter, which is convenient for realtime control, but the setting of proportional value depends on engineering experience. Setting reasonable proportional value can achieve better control, and unreasonable setting will lead to overcharge and overdischarge of energy storage components, which is harmful to the life of batteries and supercapacitors.

In order to find the optimal proportion value, traversing the different proportion values in a certain range will result in different comprehensive conversion costs. When the ratio is less than 0.42, the supercapacitor SOC will exceed the limit and cannot calculate its objective function; when the ratio is greater than 0.42, the objective function increases monotonously. The optimal ratio is 0.42.

Fig. 11 is the power curve of the battery obtained by the proportional method, and the ratio is 0.42.

OPC (0.42) is compared with DPC and PSC. The system efficiency and battery life are compared, and the percentage of optimization degree of each index is calculated as TABLE II.

V. CONCLUTION

In this paper, power distribution in HESS is optimized based on pseudo-spectral method. According to the optimized results, a real-time multi-mode DPC strategy is proposed.

Taking the typical power curves between two stations on a certain line of tramcar as an example, the pseudo-spectral method is used to calculate the power distribution ratio, so that the tramcar can complete the optimal control, and the DPC is extracted from the optimized results. By comparing the efficiency and battery life index of OPC, PSC and DPC, it is shown that the efficiency of DPC proposed in this paper is 6.83% higher than that of OPC, the battery life is 47.85% longer than that of OPC. It has obvious advantages, which is close to the optimal control PSC. By analyzing the influence of initial conditions and traffic congestion conditions on the optimal power distribution of trams, an self-adaption DPC with different working conditions is proposed, which makes the control strategy more practical.

ACKNOWLEDGMENT

This work is supported by Beijing Jiaotong University, and CRRC Qingdao Sifang Co.,Ltd.

REFERENCES

[1] X. Hu, N. Murgovski, L. M. Johannesson, and E. Bo, "Comparison of Three Electrochemical Energy Buffers Applied to a Hybrid Bus Powertrain With Simultaneous Optimal Sizing and Energy Management," *IEEE Transactions on Intelligent Transportation Systems,* vol. 15, no. 3, pp. 1193-1205, 2014.

[2] J. Shen and A. Khaligh, "Design and Real-Time Controller Implementation for a Battery-Ultracapacitor Hybrid Energy Storage System," *IEEE Transactions on Industrial Informatics,* vol. 12, no. 5, pp. 1910-1918, 2016.

[3] J. Moreno, M. E. Ortúzar, and J. W. Dixon, "Energy-management system for a hybrid electric vehicle, using ultracapacitors and neural networks," *IEEE Transactions on Industrial Electronics,* vol. 53, no. 2, pp. 614-623, 2006.

[4] N. J. Schouten, M. A. Salman, and N. A. Kheir, "Fuzzy logic control for parallel hybrid vehicles," *IEEE Transactions on Control Systems Technology,* vol. 10, no. 3, pp. 460-468, 2002.

[5] J. Shen, S. Dusmez, and A. Khaligh, "Optimization of Sizing and Battery Cycle Life in Battery/Ultracapacitor Hybrid Energy Storage Systems for Electric Vehicle Applications," *Industrial Informatics IEEE Transactions on,* vol. 10, no. 4, pp. 2112-2121, 2014.

[6] J. Shen and A. Khaligh, "Predictive control of a battery/ultracapacitor hybrid energy storage system in electric vehicles," in *Transportation Electrification Conference & Expo*, 2016.

[7] R. Carter, P. J. Hall, and A. Cruden, "Optimizing for Efficiency or Battery Life in a Battery/Supercapacitor Electric Vehicle," *IEEE Transactions on Vehicular Technology,* vol. 61, no. 4, pp. 1526-1533, 2012.

[8] V. Herrera, A. Milo, H. Gaztañaga, I. Etxeberria-Otadui, I. Villarreal, and H. Camblong, "Adaptive energy management strategy and optimal sizing applied on a battery-supercapacitor based tramway," *Applied Energy,* vol. 169, pp. 831-845, 2016.

[9] V. I. H. Pérez, H. Gaztañaga, A. Milo, A. Saez-De-Ibarra, I. Etxeberria-Otadui, and T. Nieva, "Optimal Energy Management and Sizing of a Battery Supercapacitor based Light Rail Vehicle with Multi-objective approach," *IEEE Transactions on Industry Applications,* vol. 52, no. 4, pp. 3367-3377, 2016.

[10] F. Akar, Y. Tavlasoglu, and B. Vural, "An Energy Management Strategy for a Concept Battery/Ultracapacitor Electric Vehicle with Improved Battery Life," *IEEE Transactions on Transportation Electrification,* vol. 3, no. 1, pp. 191-200, 2017.

[11] W. Zhang, J. Li, L. Xu, M. Ouyang, and Management, "Optimization for a fuel cell/battery/capacity tram with equivalent consumption minimization strategy," *Energy Conversion,* vol. 134, pp. 59-69, 2017.

[12] Y. He, Z. Chen, M. Li, and C. Ma, "Utility Function-Based Real-Time Control of A Battery Ultracapacitor Hybrid Energy System," *IEEE Transactions on Industrial Informatics,* vol. 11, no. 1, pp. 220-231, 2015.

[13] R. A. Dougal, S. Y. Liu, and R. E. White, "Power and life extension of battery-ultracapacitor hybrids," *IEEE Transactions on Components Packaging Technologies,* vol. 25, no. 1, pp. 120-131, 2002.

[14] D. Iannuzzi and P. Tricoli, "Optimal control strategy of onboard supercapacitor storage system for light railway vehicles," in *IEEE International Symposium on Industrial Electronics*, 2010.

[15] T. Mesbahi, F. Khenfri, N. Rizoug, P. Bartholomeus, and P. Le Moigne, "Combined Optimal Sizing and Control of Li-Ion Battery/Supercapacitor Embedded Power Supply Using Hybrid Particle Swarm-Nelder-Mead Algorithm," *IEEE Transactions on Sustainable Energy*.

[16] Z. Song, H. Hofmann, J. Li, X. Han, and M. Ouyang, "Optimization for a hybrid energy storage system in electric vehicles using dynamic programing approach," *Applied Energy,* vol. 139, pp. 151-162, 2015.

[17] S. Wei, Z. Yuan, F. Sun, and O. Christopher, "A pseudospectral method for solving optimal control problem of a hybrid tracked vehicle," *Applied Energy,* 2016.

[18] M. A. Patterson and A. V. Rao, "GPOPS-II: A MATLAB Software for Solving Multiple-Phase Optimal Control Problems Using hp-Adaptive Gaussian Quadrature Collocation Methods and Sparse Nonlinear Programming," *Acm Transactions on Mathematical Software,* vol. 41, no. 1, pp. 1-37, 2010.

[19] C. C. Lin, H. Peng, J. W. Grizzle, and J. M. Kang, "Power management strategy for a parallel hybrid electric truck," *IEEE Transactions on Control Systems Technology,* vol. 11, no. 6, pp. 839-849, 2004.

[20] I. Bloom *et al.*, "An accelerated calendar and cycle life study of Li-ion cells," *Journal of Power Sources,*vol. 101, no. 2, pp. 238-247, 2001.

[21] WANG *et al.*, "Cycle-life model for graphite-LiFePO4 cells," *Journal of Power Sources,*vol. 196, no. 8, pp. 3942-3948, 2011.

[22] TAKAMI *et al.*, "High-power and long-life lithium-ion batteries using lithium titanium oxide anode for automotive and stationary power applications," *Journal of Power Sources,* vol. 244, no. 4, pp. 469-475, 2013.